Chemistry & Biology, Volume *21*

Supplemental Information

Large-Scale Identification and Analysis of Suppressive Drug Interactions

Murat Cokol, Zohar B. Weinstein, Kaan Yilancioglu, Murat Tasan, Allison Doak, Dilay Cansever, Beste Mutlu, Siyang Li, Raul Rodriguez-Esteban, Murodzhon Akhmedov, Aysegul Guvenek, Melike Cokol, Selim Cetiner, Guri Giaever, Ivan Iossifov, Corey Nislow, Brian Shoichet, and Frederick P. Roth

Large-scale identification and analysis of suppressive drug interactions

Supplementary Information

Table of contents

1. Description of Supplementary Tables

Supplementary Table S1, related to experimental procedures. Suppressive drug interactions learned from literature.

Supplementary Table S2, related to Figures 1, 2, 3, 4. Raw cell growth measurements for 245 drug-drug interaction assays analyzed during this study. Each file contains a matrix of 64 columns with OD_{595} readings for one drug-drug interaction. Rows correspond to different time points with 15 minutes intervals that span 20-24 hours. Columns correspond to the 8×8 matrix of drug concentration combinations.

Supplementary Table S3, related to Figures 2, 3, 4. Growth level and suppressive drug interaction region tables for each drug interaction experiment.

Supplementary Table S4, related to Figure 5. Sensitivity scores for 5696 strains obtained for Bro_{IC20}, Sta_{IC20} and Com_{IC20} conditions.

Supplementary Table S5, related to Figure 6. Raw cell growth measurements for data represented in Figure 6d.

2. Literature curation result experimental verification

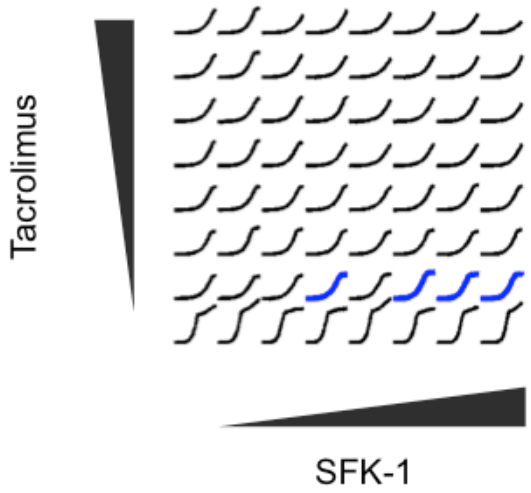

Figure S1, related to Table 1. Drug interaction experiment for SFK-1 and Tacrolimus.
SFK-1 suppresses Tacrolimus under 0.2M NaCl. The suppression can be seen by comparing the bottom two rows of the drug combination matrix. With increasing levels of Tacrolimus, presence of low doses of SFK-1 has a protective effect on Tacrolimus growth inhibition. The concentration combinations where SFK-1 suppresses Staurosporine are shown with blue growth curves.

2. Identification of suppressive drug interactions

2.1. Concentration and growth normalization

Each drug interaction experiment consists of an 8 × 8 collection of growth curves. The areas under each growth curve are computed to give an 8 × 8 "summarized growth" matrix. Drug titrations were all performed uniformly between zero drug and that drug's MIC, thus we will represent the concentrations of each drug *A* in such an experiment as one of eight values: $\frac{0}{7}\text{MIC}_A$, $\frac{1}{7}\text{MIC}_A$, … $\frac{7}{7}\text{MIC}_A$.

For each summarized growth matrix involving drug-pair *A* and *B*, growth rates (i.e. matrix values) are normalized to values ranging between 0 (MIC drug/no growth) and 1 (no-drug/full growth)[1]. Normalized (observed) growth rates for an experiment involving drug-pair *A* and *B* will be represented like so: $g_{A,B}(i_A, j_B)$ where *i* and *j* are integers between 0 and 7 (inclusive) corresponding to $\frac{i}{7}\text{MIC}_A$ and $\frac{j}{7}\text{MIC}_B$, respectively.

2.2. Self-experiments' theoretical repeats

In Cokol et al (Cokol *et al*, 2011), 25 drugs were tested against themselves, in a series of "self-experiments". Our uniform titration of drug concentrations allowed for multiple cells in each such self-experiment's summarized growth matrix to hold observed growths at the same drug concentration. These cells thus serve as repeat measurements, from which we can model the (combined technical and biological) noise in our experimental system.

As an example, consider a single self-experiment for drug *A*. For a combined concentration of $\frac{6}{7}\text{MIC}_A$ there are 7 growth measurements:

$$g_{A,A}(0_A,6_A),\ g_{A,A}(1_A,5_A),\ g_{A,A}(2_A,4_A),\ g_{A,A}(3_A,3_A),\ g_{A,A}(4_A,2_A),\ g_{A,A}(5_A,1_A),\ \text{and}\ g_{A,A}(6_A,0_A).$$

We can then take the average and the standard deviation of growth of these 7 measurements, allowing us to observe the experimental variance as a function of the mean growth.

Each self-experiment (for arbitrary drug *A*) provides 13 different combined concentrations for which repeated measurements are made, ranging between $\frac{1}{7}\text{MIC}_A$ and $\frac{13}{7}\text{MIC}_A$. (Concentrations of $\frac{0}{7}\text{MIC}_A$, and $\frac{14}{7}\text{MIC}_A$ only have one combination each, preventing repeat measurements.) Thus we have 325 such repeated average-vs-SD values (13 concentrations for each of 25 drugs), all of which are shown in Supplementary Figure 1.

2.3. Heteroskedasticity, LOESS fit, and calling significant deviations

The SD-vs-average growth repeat values in Supplementary Figure 1 show higher variance for growth values near 0.5 and lower variance near the boundary growth values of 0 and 1. This results in part[2] due to the calculation for average growth itself: since each individual growth measurement contributing to the average is bounded between 0 and (approximately) 1, averages near the boundary necessarily involve values close to the average result. We modeled this heteroskedastic relationship using a LOESS

[1] Due to experimental biological variance, it is possible to observe summarized growth rates slightly greater than 1 using this scheme; we observe these cases only a few times in our data, with values quite close to 1.

[2] In addition to any increased experimental variance at the concentrations where a drug's efficacy is near $\frac{1}{2}$ MIC, which in dose response curves is often a region of greatest variance (i.e. steepest slope).

algorithm (Cleveland & Devlin, 1988), with the results of the fit seen in Supplementary Figure 1. The 95% confidence interval (CI) of the fit was also computed, and we elected to (proceed conservatively and) take the upper boundary of this 95% fit-CI to be our modeled experimental SD as a function of some theoretical (or expected) growth g: $\sigma(g)$.

We use this value as a parameter for calling observed growth rates as being "significantly" greater than a theoretical (or expected) value, while controlling for the type-I error rate of these calls. Given a theoretical growth $\hat{g}$ for which observed growth rates will be compared against, we find the 95% quantile of the Gaussian $N(\hat{g},\sigma(\hat{g}))$ distribution, corresponding to a 5% type-I error rate (controlling for $P < 0.05$). A threshold function $g^*(\hat{g})$ is then defined as:

$$g^*(\hat{g}) = \hat{g} + Q_{0.95}(N(\hat{g},\sigma(\hat{g})))$$

where $Q(\cdot)$ is the quantile function. If any observed growth rate $g^{obs} > g^*(\hat{g})$, then we deem g^{obs} to be significantly greater than $\hat{g}$. This empirically-derived threshold can be seen as the shaded region in Supplementary Figure 2.

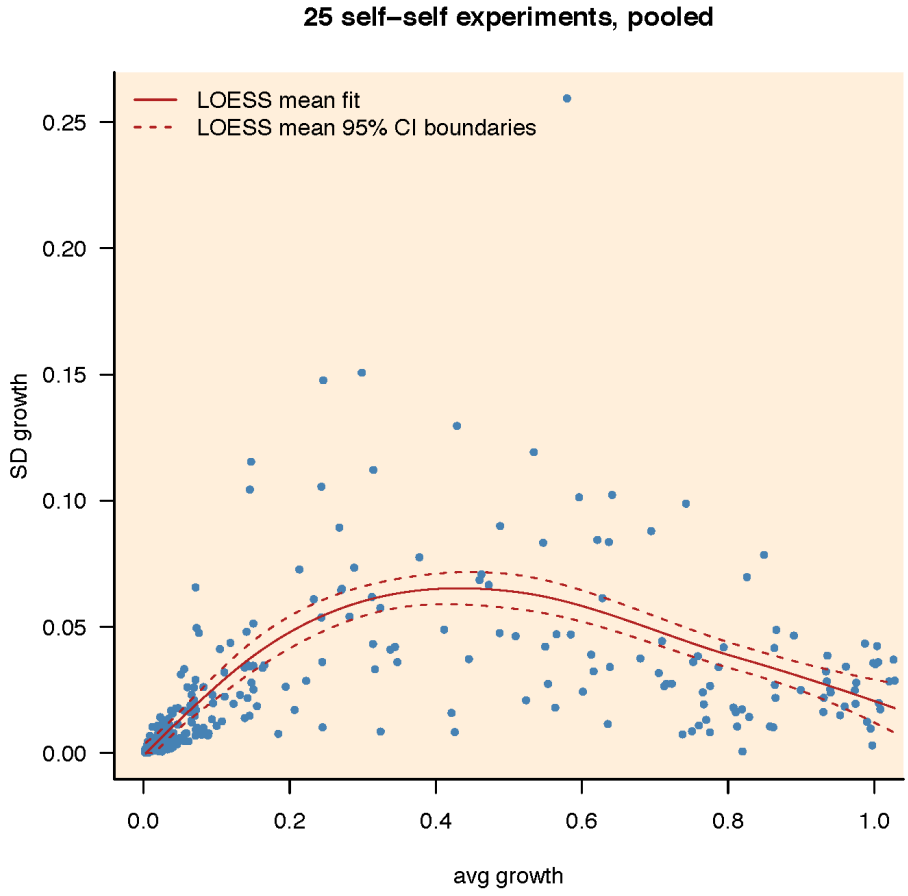

Figure S2, related to Figure 1. LOESS fit for self-experiment repeat measurement data.
Each data point represents a set of "theoretical" repeated measurements (i.e. identical concentration combinations) from the same self-experiment. Dotted lines indicate the 95% CI of the model fit.

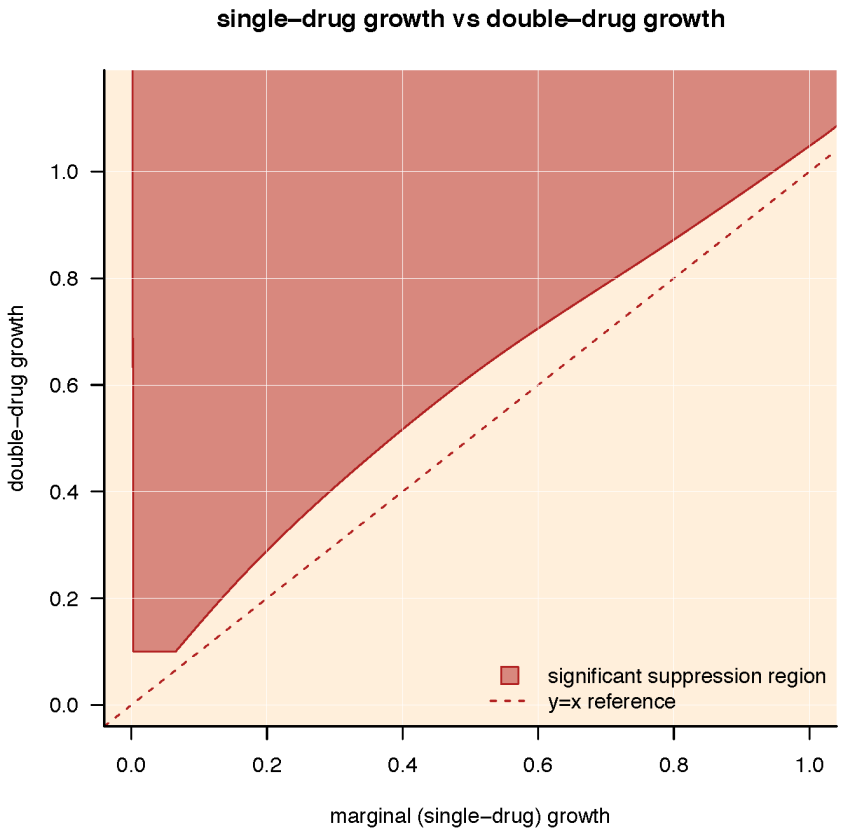

Figure S3, related to Figure 1. Suppression region shown graphically.
The x-axis represents the theoretical (or expected) growth rate and the observed (double-drug) growth rate is plotted against the y-axis. If the double-drug growth falls into the shaded region for its corresponding x-axis value, then that growth in double drug is significantly larger than the single drug growth.

2.4. Significant suppression

For any double-drug experiment with drugs *A* and *B*, we say that *A suppresses B* at concentration-combination (i_A, j_B) if:

- $g_{A,B}(i_A, j_B) > g^*(g_{A,B}(0_A, j_B))$ and
- $g_{A,B}(i_A, j_B) > g^*(g_{A,B}(0_A, j_B) \cdot g_{A,B}(i_A, 0_B))$ and
- $g_{A,B}(i_A, j_B) > 0.1$.

(We alternatively may say that *B is suppressed* by *A* (at that concentration-combination).) Such points will fall into the shaded region of Supplementary Figure 2, which we call the "significant suppression region."

For each drug-pair, we tested for all '*A* suppressing *B*' and '*B* suppressing *A*' cases, at all concentration-combinations (i_A, j_B). As an example, results of tests for 2 drug-pairs for all concentration-combinations can be seen (plotted against the significant suppression region) in the Supplementary Figure 3. Plots for all 240 experiments are available upon request.

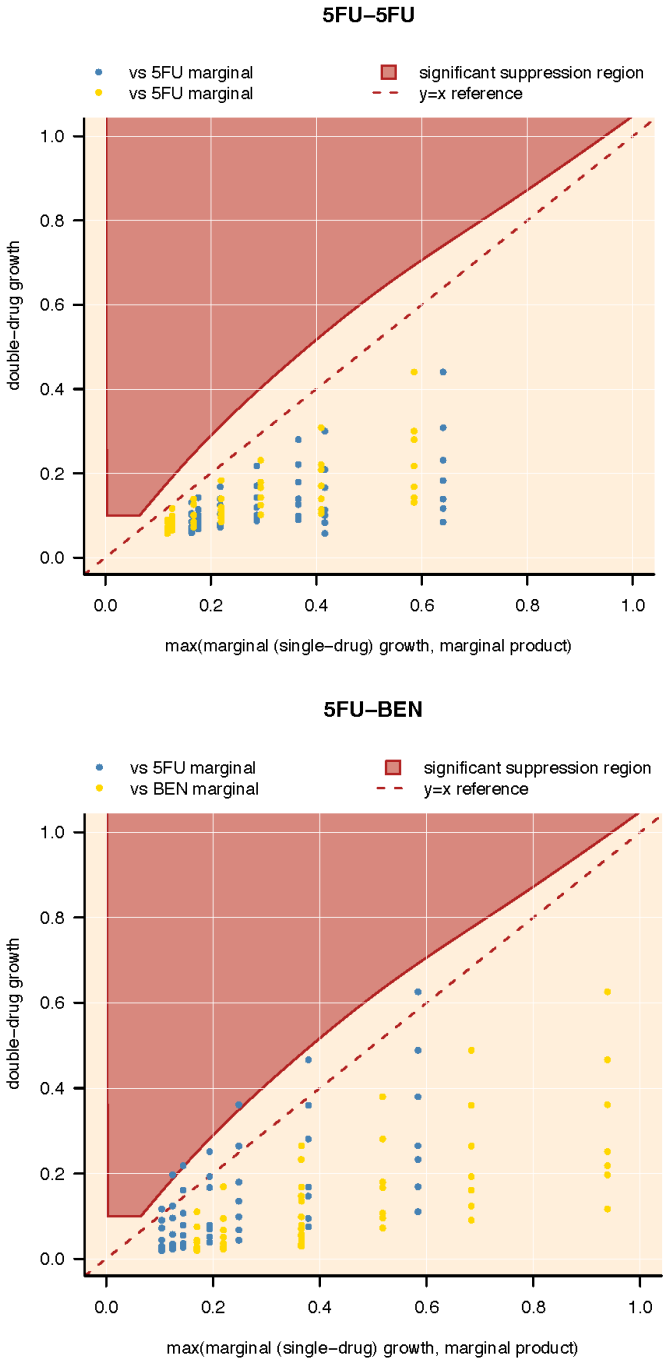

Figure S4, related to Figure 2. Results of suppression tests for two drug pairs.

Each blue and yellow dot represents the observed growth levels for one drug concentration combination. The y-values of dots correspond to the growth level in drug combination. The x-values of dots correspond to the maximum of growth level in a single drug concentration and the expected growth level in drug combination. When the y-value is significantly higher than the x-value (falling to the shaded region), suppression of the drug shown in the marginal is concluded. According to the top plot, there is no suppression relationship between 5FU and 5FU, as expected. According to the bottom plot, Ben significantly suppresses 5FU in three concentration combinations.

3. Identification of suppression hubs

For both the “initial 200" (drug interaction data reported in (Cokol et al., 2011)) and the “all 240" (drug interaction data reported in (Cokol et al., 2011) united by drug interaction data produced within this study) experiments, we handled the issue of testing multiple hypotheses using an empirical false discovery rate method. Briefly, the false discovery rate (FDR) for a set of hypotheses (usually the rejected nulls) is the proportion of those hypotheses that we expect to actually come from the null distribution (i.e. *false* rejections).

(Benjamini & Hochberg, 1995) and (Storey, 2002) give the reader a good background to the topic, and provide fast methods for FDR estimation when the hypotheses are independent and the null distribution for each hypothesis tested is U(0; 1), i.e. uniform over the range of p-values. Fisher's exact test for contingency tables -a permutation method- does not provide such a uniform null, however, and we used a simulation-based method to estimate FDRs.

3.1 Null distribution simulations

For each set of drug-drug tests, we tested two hypotheses per drug X: that drug X is a frequent suppressor, and that drug X is frequently suppressed. Each test was made using a contingency table, and to simulate the null distribution, for each such test we sampled 100,000 random contingency tables using the same marginals as the observed case. Contingency table sampling was performed using the hypergeometric distribution, and each random table was then subjected to the identical one-sided Fisher's exact test as the observed case, giving 100,000 null p-values. The null p-values were then pooled for each hypothesis in the experiment, giving 6.6×10^{-4} and 8.6×10^{-4} null p-values per experiment (respectively, for the “initial 200” and “full 240” experiments). The distributions of these simulated null p-values, layered with the distribution of observed p-values, can be seen in Supplementary Figures 4 and 5.

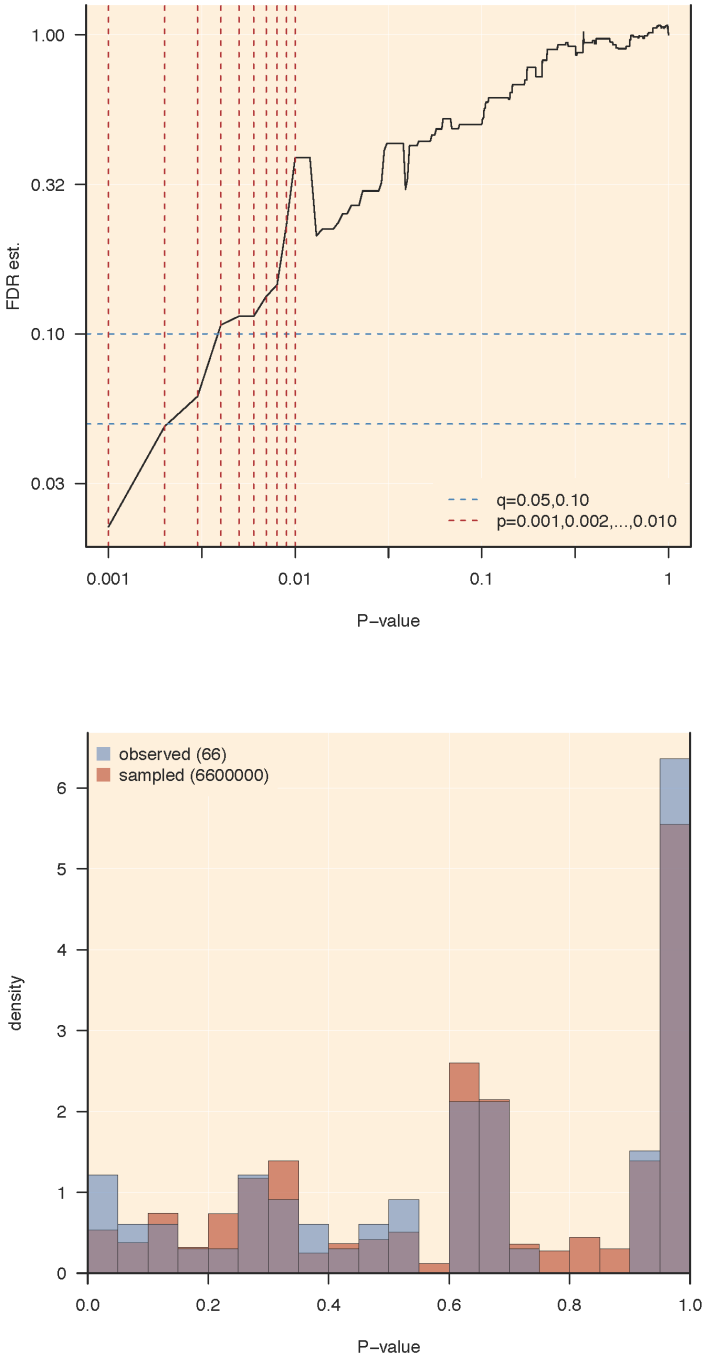

Figure S5, related to Figure 3**.** FDR estimate analysis for the "first 200" experiment batch.
Top plot shows the p-value vs FDR estimate (q-value); dotted lines show various canonical p-value and q-value cutoffs; both axes are on log scale. Bottom plot shows two overlapping histograms; blue histogram shows the distribution of observed p-values from the "first 200" experiments; red histogram shows results of 10^5 null hypothesis simulations per observed p-value. Violet is where red and blue histograms overlap.

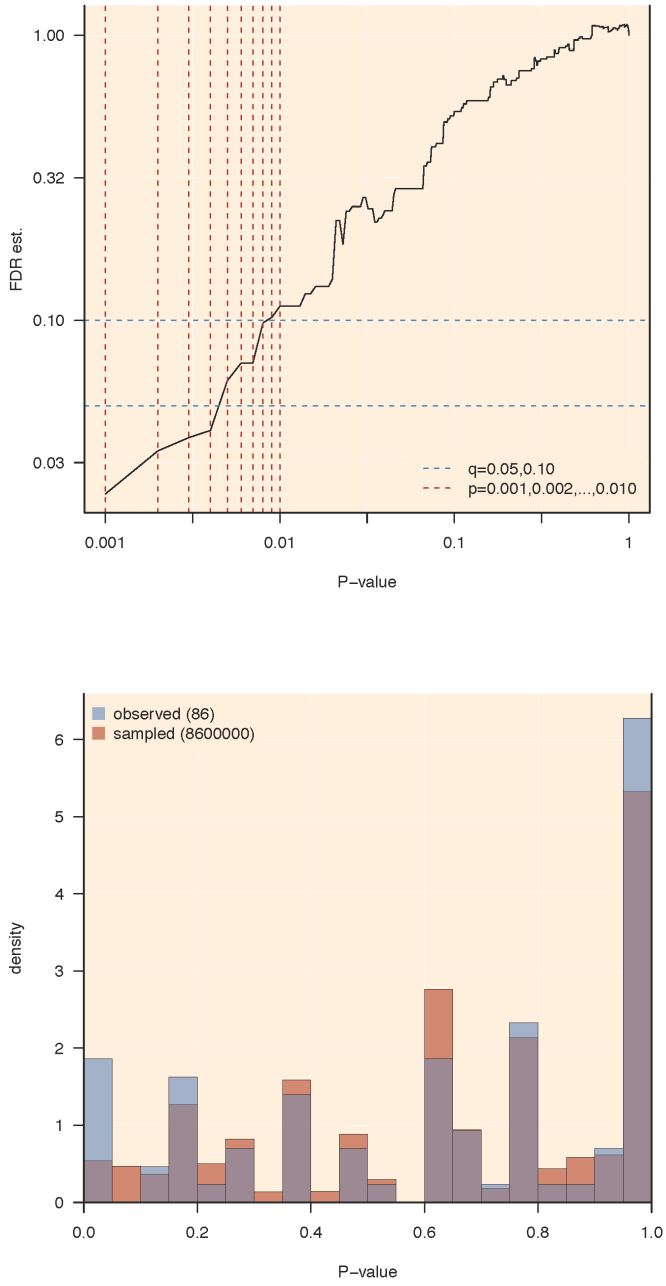

Figure S6, related to Figure 4. FDR estimate analysis for the "all 240" experiment batch.
Top plot shows the p-value vs FDR estimate (q-value); dotted lines show various canonical p-value and q-value cutoffs; both axes are on log scale. Bottom plot shows two overlapping histograms; blue histogram shows the distribution of observed p-values from the "all 240" experiments; red histogram shows results of 10^5 null hypothesis simulations per observed p-value. Violet is where red and blue histograms overlap.

3.2 FDR estimation

Given a distribution of null p-values, we estimate the FDR for the set of hypotheses with p-value smaller than p as:

$$\frac{\#_i(N_i < p) / |N|}{\#_i(O_i < p) / |O|},$$

where N is the set of null p-values, O is the set of observed p-values, and $\#_i(X_i < p)$ is the number of values in X that are less than p. In many formulations of FDR estimates, the numerator of the above equation is reduced by a value $0 < \lambda < 1$, reflecting an estimate of the number of true nulls in the full observed distribution, but traditional methods for estimating λ rely on a uniform null distribution, and thus we exclude it here (thus keeping our estimate on the conservative side).

4. Dynamic Light Scattering Experiments

To compare compound co-aggregation and suppressive drug interactions, we analyzed a set of 9 drugs (*Bro*, *Dyc*, *Fen*, *Hal*, *Rap*, *Sta*, *Tac*, *Ter* and *Tun*), both alone and in pairwise combinations in which drug suppression was observed (10 pairs: *Bro+Hal*, *Bro+Sta*, *Bro+Rap*, *Bro+Tac*, *Dyc+Fen*, *Dyc+Tun*, *Fen+Ter*, *Fen+Tun*, *Hal+Tun*, *Rap+Tac*). Single and combined drugs were prepared at the reported MIC concentrations for each drug, in exactly the same media conditions that were used for drug interaction experiments, excepting the addition of cells. We estimated the mean radius of the aggregates in each condition by using Dynamic Light Scattering (DLS) (Coan & Shoichet, 2008). Two independent replicate estimates for aggregate radius measurements had a very high correlation ($r = 0.95$, $p < 2.2\times10^{-16}$), indicating the reproducibility of our measurements. As a measure of compound precipitation at given concentration levels for each drug alone and in combination, we used the mean of these replicates. The results of this experiment are shown in Supplementary Table S6.

Drug-pair	Drug1	R (nm)	Drug2	R (nm)	Drug1+Drug2	R (nm)	Suppression
1	Bro	7	Rap	6	Bro+Rap	6	Bro suppresses Rap
2	Bro	7	Sta	6	Bro+Sta	6	Bro suppresses Sta
3	Fen	6	Ter	20	Fen+Ter	20	Ter suppresses Fen
4	Fen	6	Tun	9	Fen+Tun	7	Fen suppresses Tun
5	Bro	7	Hal	52	Bro+Hal	52	Bro suppresses Hal
6	Bro	7	Tac	335	Bro+Tac	343	Bro suppresses Tac
7	Dyc	40	Fen	6	Dyc+Fen	52	Dyc suppresses Fen
8	Dyc	40	Tun	9	Dyc+Tun	64	Dyc suppresses Tun
9	Hal	52	Tun	7	Hal+Tun	70	Hal suppresses Tun
10	Rap	6	Tac	335	Rap+Tac	314	Tac suppresses Rap

Table S6, related to Experimental Procedures. Mean aggregate radius of 10 drug pairs individually or in combination**.**

The negative control (solvent) showed an R score of 7nm. Shown in pink are individual drugs or combinations that do not aggregate (scores smaller than 40).

According to these results, 4 drug pairs (*Bro+Rap, Bro+Sta, Fen-Ter, Fen-Tun*) do not show aggregates neither individually nor in combination, therefore ruling out a co-aggregation based mechanism for the observed drug suppression. In each case of the remaining pairs, one drug does not show aggregation individually, but the other drug does, as well as the combination. In order to test if the non-aggregating compound in these cases increases the aggregation of the aggregating compound, we checked aggregation in lower dose combinations in the 6 pairs. The results of these experiments are shown in Supplementary Table S7. A comparison of the individual and combined drug aggregation in each of these cases reveals no strong indication that the non-aggregating compound is effecting the aggregation of the aggregating compound.

	Hal (ug/ml)	0.1	1	8	16	24	32	40	48	56	
	R (nm)	4.75	4.25	6.5	14.8	25.65	39.45	53.75	62.6	70.75	
	Tac (ug/ml)	1	2	4	8	16	31	47	63	79	94
	R (nm)	4.2	4.85	3.85	4.45	12.55	96.8	229.4	317.55	253.95	296.1
	Dyc (ug/ml)	1	7	14	21	28	35	42	49		
	R (nm)	4.05	6.8	8.3	14	38.35	48.6	50.65	84.25		
Bro+Hal	Hal (ug/ml)	0.1	1	8	16	24	32	40	48	56	
	Bro (ug/ml)	1	10	70	140	210	280	350	420	490	
	R (nm)	5.1	4.85	6.35	9.1	26.65	48	60.1	38.95	75.75	
Bro+Tac	Tac (ug/ml)	1	2	4	8	16	31	47	63	79	94
	Bro (ug/ml)	4.8	8.8	17.5	35	70	140	210	280	350	420
	R (nm)	5.15	4.3	3.9	4.2	11.35	122.25	231.8	236.35	227.25	322.45
Dyc+Fen	Fen (ug/ml)	0.1	0.22	0.44	0.66	0.88	1.1	1.32	1.54		
	Dyc (ug/ml)	1	7	14	21	28	35	42	49		
	R (nm)	4.95	7.9	8.15	14.3	37.7	54.55	59.3	86.35		
Dyc+Tun	Tun (ug/ml)	0.01	0.05	0.1	0.15	0.2	0.25	0.3	0.35		
	Dyc (ug/ml)	1	7	14	21	28	35	42	49		
	R (nm)	4.65	7	8.55	15.25	33.7	57.4	59.4	89.7		
Hal+Tun	Hal (ug/ml)	0.1	1	8	16	24	32	40	48	56	
	Tun (ug/ml)	0.001	0.01	0.05	0.1	0.15	0.2	0.25	0.3	0.35	
	R (nm)	5.25	5.15	6.6	9.05	33.35	57.9	59.05	60.4	95.35	
Rap+Tac	Tac (ug/ml)	1	2	4	8	16	31	47	63	79	94
	Rap (ng/ml)	0.048	0.09	0.18	0.35	0.7	1.4	2.1	2.8	3.5	4.2
	R (nm)	4.85	4.2	4.4	4.85	9.6	50.25	37.5	359.45	287	319.85

Table S7, related to Experimental Procedures. Further DLS experiment results to test co-aggregation in aggregating drugs.

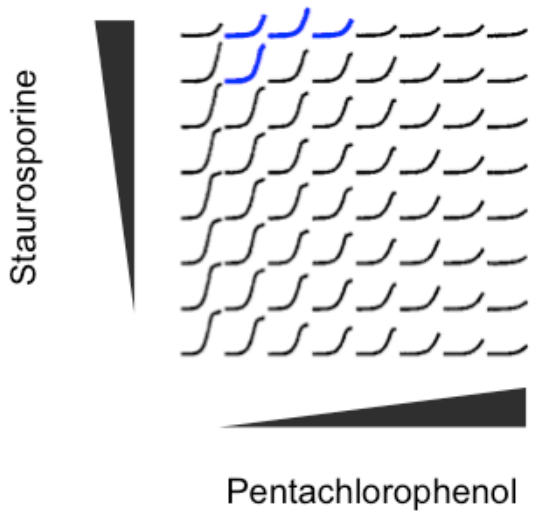

Figure S7, related to Figure 6. Pentachlorophenol, a weak base and an oxidative phosphorylation inhibitor, suppresses Staurosporine. The concentration combinations where Pentachlorophenol suppresses Staurosporine are shown with blue growth curves.

References

Benjamini Y & Hochberg Y (1995) Controlling the false discovery rate: a practical and powerful approach to multiple testing. *J R Stat Soc Series B Stat Methodol***:** 289–300

Cleveland WS & Devlin SJ (1988) Locally weighted regression: An approach to regression analysis by local fitting. *J Am Stat Assoc* **83:** 596–610

Coan KED & Shoichet BK (2008) Stoichiometry and physical chemistry of promiscuous aggregate-based inhibitors. *J. Am. Chem. Soc.* **130:** 9606–9612

Cokol M, Chua HN, Tasan M, Mutlu B, Weinstein ZB, Suzuki Y, Nergiz ME, Costanzo M, Baryshnikova A, Giaever G, Nislow C, Myers CL, Andrews BJ, Boone C & Roth FP (2011) Systematic exploration of synergistic drug pairs. *Mol. Syst. Biol.* **7:** 544

Storey JD (2002) A direct approach to false discovery rates. *J R Stat Soc Series B Stat Methodol* **64:** 479–498